Domain analysis of Kv6.3, an electrically silent channel

Natacha Ottschytsch[1], Adam L. Raes[1], Jean-Pierre Timmermans[2] and Dirk J. Snyders[1]

[1] *Laboratory for Molecular Biophysics, Physiology and Pharmacology, Department of Biomedical Sciences, University of Antwerp, Belgium*
[2] *Laboratory of Cell Biology and Histology, Department of Biomedical Sciences, University of Antwerp, Belgium*

The subunit Kv6.3 encodes a voltage-gated potassium channel belonging to the group of electrically silent Kv subunits, i.e. subunits that do not form functional homotetrameric channels. The lack of current, caused by retention in the endoplasmic reticulum (ER), was overcome by coexpression with Kv2.1. To investigate whether a specific section of Kv6.3 was responsible for ER retention, we constructed chimeric subunits between Kv6.3 and Kv2.1, and analysed their subcellular localization and functionality. The results demonstrate that the ER retention of Kv6.3 is not caused by the N-terminal A and B box (NAB) domain nor the intracellular N- or C-termini, but rather by the S1–S6 core protein. Introduction of individual transmembrane segments of Kv6.3 in Kv2.1 was tolerated, with the exception of S6. Indeed, introduction of the S6 domain of Kv6.3 in Kv2.1 was enough to cause ER retention, which was due to the C-terminal section of S6. The S4 segment of Kv6.3 could act as a voltage sensor in the Kv2.1 context, albeit with a major hyperpolarizing shift in the voltage dependence of activation and inactivation, apparently caused by the presence of a tyrosine in Kv6.3 instead of a conserved arginine. This study suggests that the silent behaviour of Kv6.3 is largely caused by the C-terminal part of its sixth transmembrane domain that causes ER retention of the subunit.

(Resubmitted 23 June 2005; accepted after revision 5 August 2005; first published online 11 August 2005)
Corresponding author D. J. Snyders: Laboratory for Molecular Biophysics, Physiology and Pharmacology, Department of Biomedical Sciences, University of Antwerp (CDE), Universiteitsplein 1, T4.21, 2610 Antwerp, Belgium. Email: dirk.snyders@ua.ac.be

Voltage-gated potassium channels serve a wide range of functions including regulation of the resting membrane potential and control of the shape, duration and frequency of action potentials (Barry & Nerbonne, 1996; Pongs, 1999; Hille, 2001). These channels are transmembrane proteins consisting of at least four α-subunits which form a central selective permeation pathway for K^+ ions. Each α-subunit contains six transmembrane domains (S1–S6) and a pore loop between S5 and S6 which contains the GYG-motif, the signature sequence for potassium selectivity (Heginbotham *et al.* 1994). The fourth transmembrane domain (S4) contains positively charged residues and is the major part of the voltage sensor. This domain detects a change in voltage across the membrane and its movement causes a conformational change in the channel, thereby opening or closing the channel (Bezanilla, 2000). We recently cloned three subunits belonging to the *Shaker*-type Kv family of potassium channels, designated Kv6.3, Kv10.1 and Kv11.1, based on the degree of homology with other *Shaker*-type channels (Ottschytsch *et al.* 2002) (The IUPHAR gene nomenclature committee later placed Kv10.1 and Kv11.1 as members of the Kv6 and Kv8 subfamilies, respectively, and renamed Kv6.3 to Kv6.4). The subunits of the Kv1 to Kv4 subfamilies all show functional expression in a homotetrameric configuration. The subunits of the Kv5 to Kv11 are not able to generate current by themselves, despite their typical topology of voltage-gated potassium channel subunits, and are therefore often referred to as 'electrically silent' (Drewe *et al.* 1992; Hugnot *et al.* 1996; Patel *et al.* 1997; Salinas *et al.* 1997*b*; Zhu *et al.* 1999; Ottschytsch *et al.* 2002). All known electrically silent subunits have been shown to form heterotetrameric channels with the members of the Kv2 subfamily (Salinas *et al.* 1997*b*; Patel *et al.* 1999; Zhu *et al.* 1999; Ottschytsch *et al.* 2002). Expression of these heterotetrameric channels resulted in currents with properties that are usually clearly distinguishable from wild-type (WT) Kv2. As such, these 'silent' subunits can be considered as regulatory subunits of Kv2 channels. A physiological role for Kv6.3 has recently been demonstrated in urinary bladder smooth muscle; in this case the whole-cell $I_{K(V)}$ was consistent with heterotetrameric Kv2.1/Kv6.3 channels (Thorneloe & Nelson, 2003).

The silent subunits do not produce current by themselves, due to retention in the endoplasmatic reticulum (ER) (Salinas *et al.* 1997*a*,*b*; Shepard & Rae, 1999; Ottschytsch *et al.* 2002). Co-expression of Kv2

 DOI: 10.1113/jphysiol.2005.090142

subunits rescues the silent channels out of the ER and transports the heteromeric complex to the plasma membrane (Salinas *et al.* 1997*a*; Ottschytsch *et al.* 2002). It remains unclear why these silent channels are retained in the ER when expressed alone. Export from the ER is an important checkpoint for proteins. Misfolded or unassembled proteins are retained, often because specific (e.g. hydrophobic) sequences are exposed which are normally buried when the protein is properly folded or assembled (Zerangue *et al.* 1999; Margeta-Mitrovic *et al.* 2000). In other cases, specific retention signals retain the protein in the ER. To investigate why the silent Kv subunits are retained in the ER, we constructed chimeric channels in which domains of the functional and properly trafficking channel Kv2.1 were replaced by the corresponding domains of the silent channel Kv6.3.

Methods

Molecular biology

Human Kv2.1 and Kv6.3 (GenBank acc. no. AF348984) were both cloned into the pEGFP-N1 vector (Clontech, Palo Alto, CA, USA) allowing the green fluorescent protein (GFP) to be in frame with the channel, as such creating C-terminal GFP-tagged channels (Ottschytsch *et al.* 2002). Chimeric constructs were developed using a loop-in PCR strategy. Site-directed mutagenesis was carried out using the QuikChange method (Stratagene, La Jolla, CA, USA). All the obtained constructs were verified by DNA sequencing.

Cell culture and transfection

Ltk$^-$ cells were cultured in DMEM supplemented with 10% horse serum and 1% penicillin–streptomycin under a 5% CO_2 atmosphere. For electrophysiological experiments, Ltk$^-$ cells were transiently transfected with 0.1–5 μg GFP-tagged cDNA using LipofectAMINE reagent according to the manufacturer's instructions (Invitrogen, San Diego, CA, USA). Cells were trypsinized 12–24 h post-transfection and used for analysis within 12 h.

Whole-cell current recording

Current recordings were made with an Axopatch-200B amplifier (Axon instruments, Union City, CA, USA) in the whole-cell configuration of the patch-clamp technique (Hamill *et al.* 1981). Experiments were performed at room temperature (20–23°C) and current recordings were low-pass filtered and sampled at 2–10 kHz with a Digidata 1200A data acquisition system (Axon instruments). Command voltages and data storage were controlled with pClamp8 software (Axon Instruments). Patch pipettes were pulled with a laser puller (Sutter Instruments, Novato, CA, USA) from 1.2 mm borosilicate glass (World Precision Instruments, Sarasota, FL, USA). After heat polishing, the patch-pipettes had resistances $<$3 MΩ. The cells were continuously perfused with a bath solution containing (mM): NaCl 130, KCl 4, $CaCl_2$ 1.8, $MgCl_2$ 1, Hepes 10, Glucose 10, adjusted to pH 7.35 with NaOH. The pipettes were filled with intracellular solution containing (mM) KCl 110, K_4BAPTA 5, K_2ATP 5, $MgCl_2$ 1, Hepes 10, adjusted to pH 7.2 using KOH. Junction potentials were zeroed with the filled pipette in the bath solution. After achieving a gigaohm seal, the whole-cell configuration was achieved by mouth suction. The access resistance varied from 4 to 9 MΩ. After compensation the series resistance was kept below 3 MΩ to ensure that voltage errors were $<$5 mV.

Pulse protocols and data analysis

The applied pulse protocols are described in the figure legends. The voltage dependence of channel opening and inactivation (activation and inactivation curves) was fitted with a Boltzmann equation according to:

$$y = 1/\{1 + \exp[-(E - V_{1/2})/k]\},$$

where $V_{1/2}$ represents the voltage at which 50% of the channels are open or inactivated and k the slope factor. Activation and deactivation kinetics were fitted with a single or double exponential function using a non-linear least-squares (Gauss–Newton) algorithm. Results are presented as mean ± S.E.M.

Confocal imaging

Ltk$^-$ cells were cultivated on coverslips for 48 h and transfected with 0.5 μg GFP-tagged channel using the lipofectamine method (see above). The same amount of a red fluorescent protein containing ER targeting and retrieval sequences, DsRED-ER, was cotransfected as ER marker (Ottschytsch *et al.* 2002). After 48 h, single confocal images were obtained on a Zeiss CLSM 510, equipped with an argon laser (excitation: 488 nm) and a helium–neon laser (excitation: 543 nm) for the visualization of GFP and DsRED-ER, respectively. Images were captured with a water immersion 40× C-apochromat (NA: 1.2) lens and a zoom factor was set between 5 and 7 in all scanning sessions. The thickness of the confocal slices was 1 μm. The images (pixel resolution 512 × 512) were then further digitally processed using Zeiss LSM Image Browser and Corel PHOTO-PAINT.

Results

The trafficking behaviour of Kv6.3- and Kv2.1-containing channels was determined in Ltk$^-$ cells. Kv2.1 with GFP

fused to its C-terminus was clearly detected at the periphery of the cell, presumably the plasma membrane, and gave rise to time-dependent outward currents upon depolarization (Fig. 1). Kv6.3GFP however, was unable to produce current and was localized in intracellular compartments. The green fluorescence of Kv6.3GFP colocalized with the red fluorescence of DsRED-ER, which was cotransfected as a marker for the ER (Fig. 1). This indicates that the Kv6.3GFP subunits were trapped in the ER. In contrast, co-expression of Kv2.1 with Kv6.3GFP resulted in outward currents and green plasma membrane staining. This demonstrates that Kv2.1 was able to rescue the Kv6.3GFP subunits out of the ER (Fig. 1). These results confirm and expand previous data obtained in human embryonic kidney (HEK) cells (Ottschytsch *et al.* 2002). To determine which domain of Kv6.3 was responsible for the ER retention, we constructed several chimeric subunits in which domains of Kv6.3 and Kv2.1 were exchanged.

The NAB domain of Kv6.3

The intracellular N-terminus of Kv channels contains a N-terminal A and B box (NAB) (or T1) domain, which controls the subfamily-specific tetramerization of the subunits (Li *et al.* 1992; Shen and Pfaffinger, 1995; Xu *et al.* 1995; Papazian, 1999). Figure 2 shows an alignment of Kv2.1 and Kv6.3 demonstrating that Kv6.3 also contains the conserved NAB domain. In a previous study we demonstrated by the yeast two-hybrid approach that the amino termini of Kv6.3 were unable to interact with each other (Ottschytsch *et al.* 2002). This indicated that the NAB domain of Kv6.3, while present, might be unable to form homotetramers (or even prevent their formation). To evaluate this hypothesis we replaced the amino terminus of Kv6.3 by the amino terminus of Kv2.1 (chimera 1, Fig. 3*A*). If the retention of Kv6.3 in the ER was solely due to an incompatible NAB domain, then chimera 1 should be functional. However expression of chimera 1 did not yield voltage-dependent K^+ currents. Co-expression of the GFP-tagged chimera with DsRED-ER showed a yellow intracellular staining in the overlay, indicating colocalization of both fluorophores and thus demonstrating that the subunits were mainly trapped in the ER (Fig. 3*A*). Thus, the N-terminus of Kv2.1 was not able to restore the function of Kv6.3, demonstrating that an incompatible NAB domain is not solely responsible for the non-functionality of Kv6.3.

Does the N- or C-terminus contain trafficking signals?

Plasma membrane proteins are often selectively exported out of the ER due to short stretches of amino acids referred to as forward transport signals or ER export signals. Channels containing such a forward transport signal traffic much faster to the plasma membrane. In the case of Kv1.2 it was shown that the surface expression of the channel was greatly enhanced when it was fused to the ER export signal FCYENE from Kir channels (Ma *et al.* 2001). A simple explanation for ER retention of Kv6.3 would be the lack of export signals. To test whether the forward-trafficking signal was able to restore the function of Kv6.3 as well, the FCYENE sequence was N-terminally fused to the Kv6.3

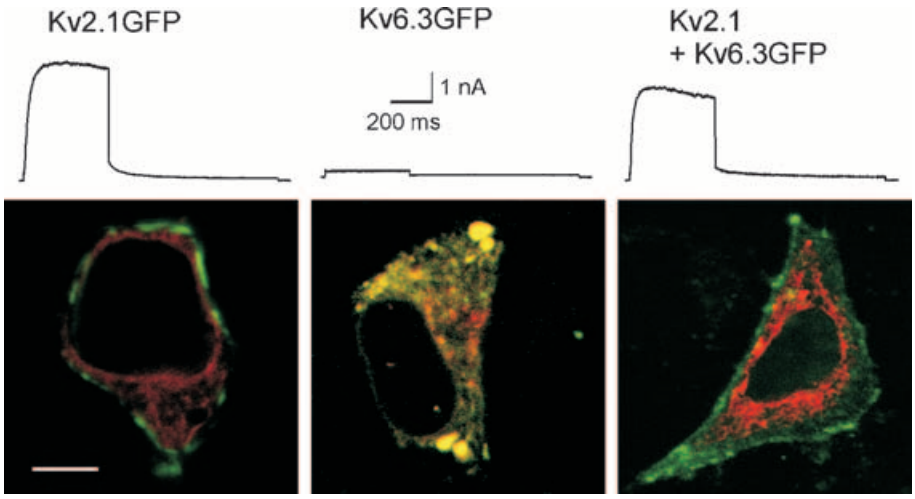

Figure 1. Whole-cell current recordings and subcellular localization of Kv2.1GFP, Kv6.3GFP and the coexpression
Currents were evoked by stepping from −80 mV to +70 mV, 500 ms in duration, followed by a repolarizing pulse at −30 mV, 1 s in duration. The scale bar applies to all traces shown. The confocal images show Ltk$^-$ cells expressing the GFP-tagged subunits and the DsRED-ER localization vector. The scale bar on the image represents 5 μm. For the co-expression, a 10 : 1 ratio of Kv2.1 and Kv6.3GFP cDNA was used.

subunit. No current was generated and Kv6.3 remained in the ER (FCYENE-Kv6.3, Fig. 3*B*).

Another reason why Kv6.3 remains in the ER could be the presence of ER retention or retrieval signals. If ER resident proteins escape the ER, retrieval signals are exposed and the proteins are retrieved into COPI-coated vesicles for retrograde transport back to the ER (Letourneur *et al.* 1994; Gaynor *et al.* 1998). Misfolded or unassembled proteins are not allowed to leave the ER due to retention signals that are exposed. In the correctly folded or fully assembled proteins these signals are hidden. Retrieval or retention signals are frequently located in the intracellular N- or C-termini of proteins. Sequence analysis of Kv6.3 revealed no well-established trafficking signals, such as KDEL. To test whether the N- or C-termini of Kv6.3 contain other ER retention or retrieval signals, we replaced both termini by those of Kv2.1, a channel that traffics very well (chimera 2, Fig. 3*B*). Nevertheless, these chimeric subunits were still retained in the ER. These results strongly suggest that the S1–S6 core of Kv6.3 causes the trafficking deficiency.

The voltage-sensing domains and the ion-conducting pore module of Kv6.3

The S1–S6 core protein of a voltage-gated Kv channel can be divided into two domains: the voltage-sensing domain (S1–S4) and the ion-conducting pore domain (S5–S6). The voltage-sensing domain senses the changes in the membrane potential, and triggers a conformational change in the protein leading to opening or closing of the ion-conducting pore domain. To test whether one of these two domains of Kv6.3 was non-functional, we introduced the voltage-sensing domain and the ion-conducting domain of Kv2.1 in a Kv6.3 background in an attempt to restore the functionality of Kv6.3 (chimeras 3 and 4). Surprisingly, both chimeras were non-functional (Fig. 3*C*). However, chimera 4 still contained the linkers of Kv6.3. It has been shown that the linkers between the transmembrane domains often contain important residues for ion channel function (Chen *et al.* 2001; Gong *et al.* 2002). Therefore, we changed the linkers in chimera 4 to Kv2.1 sequence, but this chimera 5 was still unable to traffic to the plasma membrane and remained silent (Fig. 3*C*).

Introducing single transmembrane domains and the pore loop of Kv6.3 in Kv2.1

To test whether we could identify a specific segment of the voltage-sensing and/or ion-conducting domain of Kv6.3 that causes the impaired trafficking, we introduced each transmembrane domain and the pore loop of Kv6.3 separately in a Kv2.1 background (chimeras 6–12, Fig. 4). Surprisingly, all these chimeras were functional,

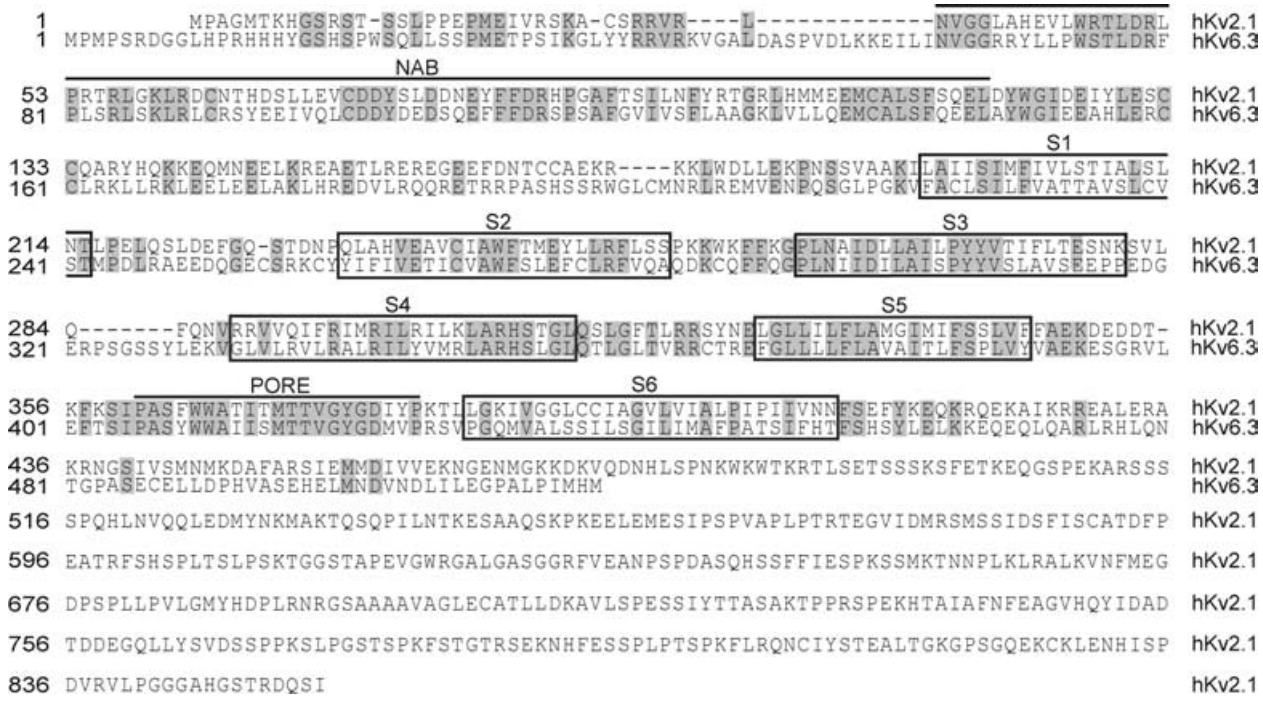

Figure 2. Alignment of Kv2.1 and Kv6.3
The amino acid sequences of Kv2.1 and Kv6.3, aligned using MEGALIGN. Gaps (indicated by dashes) were introduced in the sequence to maintain the alignment. Identical residues between Kv2.1 and Kv6.3 are shaded in grey to show the homology. The NAB domain and the pore region are indicated by an over line. The six transmembrane domains are boxed. The boundaries of the boxes were used to construct chimeras, unless indicated otherwise.

with the exception of S6 (chimera 12). Figure 4 shows the typical current traces and subcellular localization of chimeras 6–12. The pore loop of Kv6.3 (chimera 11) resulted in a functional K^+-selective channel, although we never observed a clear staining of the plasma membrane. The latter suggests that the number of channels at the level of the plasma membrane is reduced. To test whether the lack of plasma membrane staining reflects the reduced number of channels at the cell surface, the amount of current produced by the chimeras was determined by the average normalized peak amplitude of the channels (Fig. 5). Chimera 11 showed a marked reduction of current amplitude compared to the other chimeras, in agreement with the reduced staining at the level of the plasma membrane that was observed with the confocal imaging.

The biophysical properties of the functional chimeras are presented in Table 1. Compared to wild-type Kv2.1, the voltage dependence of activation of chimeras 7 (S2) and 8 (S3) was markedly altered, showing a shift of $V_{1/2}$ of −40 mV and +30 mV, respectively (Fig. 6*A*). The voltage dependence of inactivation was also shifted for both chimeras, showing a shift of −44 mV and +14 mV for chimeras 7 and 8, respectively (Fig. 6*B*). The slowing of the kinetics of activation and deactivation was most pronounced in chimeras 9 (S4) and 10 (S5) (Fig. 6*C*).

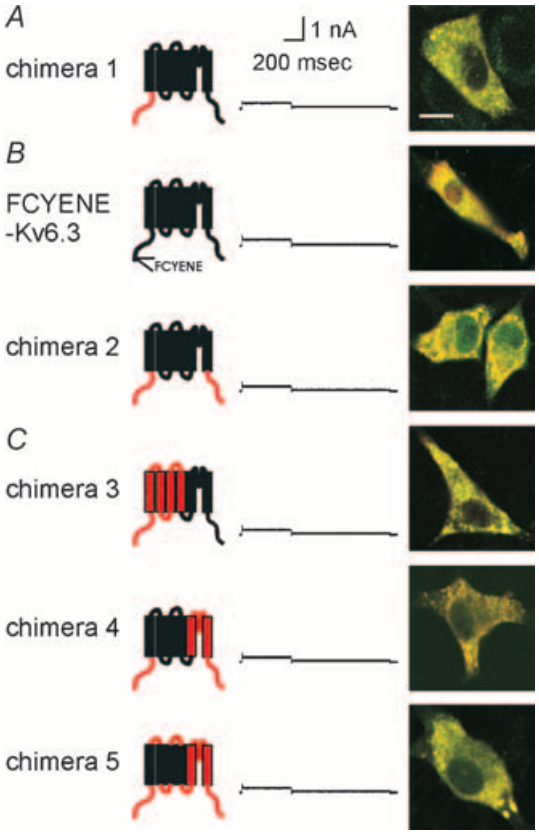

Figure 3. Subcellular localization and typical whole-cell current recording of *A*, chimera 1, *B*, FCYENE-Kv6.3 and chimera 2, C, chimeras 3–5
In the cartoon of the chimeric subunit, Kv2.1 and Kv6.3 domains are coloured red and black, respectively. This colour code is maintained throughout the figures. A typical whole-cell current recording is displayed. The holding potential was −80 mV and cells were depolarized to +70 mV, 500 ms in duration, followed by a repolarizing pulse at −30 mV, 1 s in duration. The scale bar applies to all traces shown. The confocal image shows an overlay of the GFP-tagged chimera and an ER-marker (DsRED-ER), indicating colocalization in the ER. The scale bar on the image represents 5 μm.

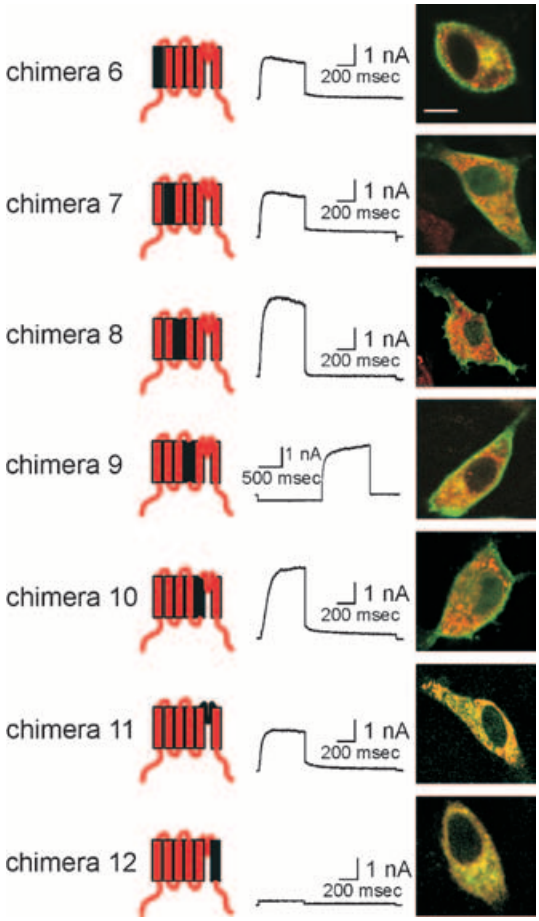

Figure 4. Subcellular localization and typical current traces of Kv2.1 chimeras containing single transmembrane domains or the pore loop of Kv6.3
Chimeras are shown on the left. Typical current recordings are displayed in the column in the middle. The holding potential was −80 mV and cells were depolarized to +70 mV, 500 ms in duration, followed by a repolarizing pulse at −30 mV, 1 s in duration. For chimera 9, the holding potential was −40 mV. A 2 s. prepulse of −120 mV was given to recover from inactivation, followed by a depolarizing step to +70 mV, 1.5 s in duration. On the right, a confocal image of an overlay of the GFP-tagged chimeras and DsRED-ER is shown, indicating clear membrane staining for chimeras 6 to 10. The scale bar on the image represents 5 μm.

Table 1. Electrophysiological parameters of Kv2.1, Kv2.1/Kv6.3 and the functional chimeras

	Voltage dependence						Time constants			
	Activation			Inactivation			Activation at 30 mV		Deactivation at −50 mV	
	$V_{1/2}$ (mV)	k (mV)	n	$V_{1/2}$ (mV)	k (mV)	n	τ_{fast} (ms)	n	τ_{fast} (ms)	n
Kv2.1	12.2 ± 1.4	9.5 ± 0.6	11	−15.9 ± 1.2	7.2 ± 0.6	5	68.4 ± 6.8	7	16.6 ± 1.1	5
+ Kv6.3	−4.2 ± 0.7	15.1 ± 0.7	5	−55.6 ± 1.1	6.6 ± 0.8	6	22.6 ± 3.2	8	35.8 ± 6.5	5
Chimera 6	−2.8 ± 1.4	11.0 ± 0.6	8	−27.3 ± 0.9	6.4 ± 0.6	6	25.9 ± 2.7	10	20.4 ± 3.1	5
Chimera 7	−27.8 ± 1.0	7.7 ± 0.3	7	−59.6 ± 2.1	6.3 ± 0.1	5	20.1 ± 2.3	8	23.7 ± 2.3	6
Chimera 8	43.6 ± 3.5	14.8 ± 0.5	7	−1.7 ± 2.7	8.1 ± 2.7	5	99.5 ± 15.9	10	7.1 ± 0.6	9
Chimera 9	ND	ND		<−120	ND		107 ± 26	5	ND	
ch9–Y306R	−0.3 ± 3.0	13.1 ± 1.0	10	−31.6 ± 2.4	7.2 ± 0.5	11	78.6 ± 11.8	8	8.3 ± 1.0	6
Chimera 10	1.1 ± 1.4	8.6 ± 0.6	9	−25.5 ± 1.0	5.6 ± 0.6	6	116.0 ± 11.9	6	32.0 ± 1.4	9
Chimera 11	3.5 ± 1.9	9.4 ± 0.5	9	−24.3 ± 1.3	5.7 ± 0.4	5	31.8 ± 5.6	7	22.6 ± 4.3	7
Chimera 14	3.6 ± 3.8	10.6 ± 1.2	5	−25.0 ± 1.2	7.5 ± 1.6	4	302.6 ± 69.0	5	140.4 ± 26.9	5
Kv2.1 + chimera 12	8.8 ± 1.2	13.1 ± 0.6	5	−25.8 ± 1.5	9.3 ± 1.0	5	59.7 ± 3.1	5	23.5 ± 4.02	6
Kv2.1 + chimera 13	15.1 ± 1.0	12.1 ± 0.5	6	−20.6 ± 0.6	7.8 ± 0.7	5	87.2 ± 5.3	6	15.4 ± 2.0	5

Values are given as mean ± S.E.M.; n = number of experiments. $V_{1/2}$ and k obtained from Boltzmann fit (see Methods). ND, not determined.

The S4 domain of Kv6.3

Chimera 9 demonstrates that the S4 segment of Kv6.3 could act as a functional voltage sensor in Kv2.1, although the voltage dependencies of activation and inactivation were shifted strongly to hyperpolarizing potentials (Fig. 4, Table 1). Therefore, we were not able to achieve complete recovery from inactivation; at −90 mV the channels were completely inactivated and the midpoint of inactivation was at least −120 mV ($n = 7$). As a consequence, the midpoint of activation was also difficult to determine, but the threshold of activation was more negative than −70 mV. The S4 segment of the Kv6 subfamily lacks an important arginine residue, which is conserved in all functional Kv channels (R371 in *Shaker*). In Kv6.3 a tyrosine is located at this position (Fig. 7*A*). To investigate whether the missing arginine caused the strongly altered voltage dependence, the tyrosine was mutated into an arginine (chimera 9–Y306R). Indeed, the voltage dependence of this chimeric subunit was shifted back towards depolarizing potentials (Table 1, Fig. 7*B*), underlining the importance of this conserved arginine in the gating of a Kv channel.

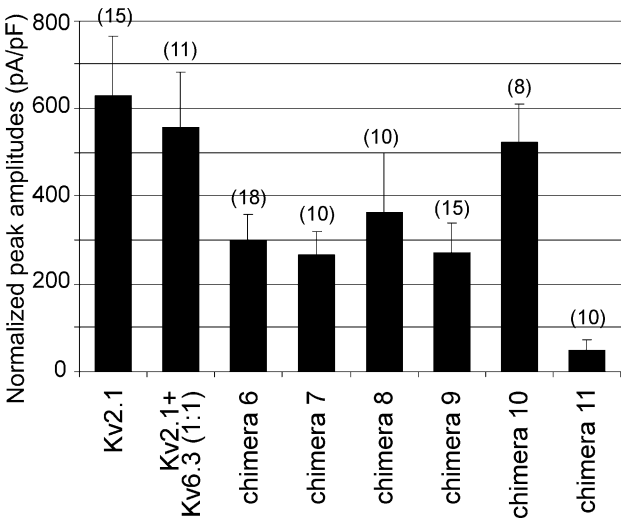

Figure 5. Histogram of peak amplitudes of Kv2.1, Kv2.1/Kv6.3 and chimeras 6–11 currents
Ltk– cells were transfected with 0.5 μg cDNA for each construct. For the cotransfection a 1 : 1 ratio was used, by transfecting 0.25 μg Kv2.1 and 0.25 μg Kv6.3. Peak amplitudes were measured by stepping from −80 mV to 70 mV and normalized to cell size. Data are shown + S.E.M. The number of cells used is indicated in parentheses for each construct.

The S6 domain of Kv6.3

The only domain of Kv6.3 that produced a non-functional chimera was S6 (chimera 12, Fig. 4). It has been suggested that the interaction of the lower part of S6 with the S4–S5 linker is part of the gating machinery of the voltage-gated potassium channel (Tristani-Firouzi *et al.* 2002; Decher *et al.* 2004). As a consequence the incompatibility of the S6 segment of Kv6.3 with the S4–S5 linker of Kv2.1 could be responsible for the non-functionality of chimera 12. Therefore, we simultaneously replaced the S4–S5 linker and the S6 segment of Kv2.1 by the Kv6.3 sequence resulting in chimera 13, which, however, was still not functional and was retained in the ER (Fig. 8*A*).

In all functional Kv channels, the lower part of S6 contains a highly conserved proline-X-proline (PXP) motif. This double proline motif is thought to cause a bend in the S6 helix and is important for channel gating (del Camino *et al.* 2000; Labro *et al.* 2003). In Kv6.3, only the first proline is present while the second

proline is replaced by a threonine (Fig. 8*B*). To evaluate the importance of this motif, we replaced the lower part of S6 (starting from the PXP motif) by the Kv2.1 sequence. The resulting chimera, which only contained the Kv6.3 sequence above the PXP motif, was clearly present in the plasma membrane (chimera 14, Fig. 8*A* and *B*). The resulting currents displayed slower activation and deactivation kinetics than Kv2.1 currents (Fig. 6*D*, Table 1).

To test whether chimeras 12 and 13 were non-functional solely because of the absence of a PXP motif, we introduced the second proline in both chimeras (chimera 12–PXP and chimera 13–PXP). These chimeras were equally non-functional, indicating that other residues in the lower part of S6 are responsible for the non-functionality of chimeras 12 and 13 (Fig. 8*A*). Salinas *et al.* (1997*a*) showed that the S6 segment of Kv8.1 is involved in the modulation of Kv2.1 by Kv8.1. To determine whether the S6 domain of Kv6.3 is similarly important for the regulatory effect of Kv6.3 on Kv2.1, we performed co-expressions of Kv2.1 with chimera 12 or 13. Confocal imaging showed that the GFP-tagged chimeras 12 and 13 were each able to interact with Kv2.1 as both chimeras were rescued out of the ER and transported to the cell surface (Fig. 8*C*). Analysis of the currents from the co-expressions showed that the voltage dependence of activation and inactivation as well as the kinetics of activation and deactivation were not substantially different from WT Kv2.1, indicating that the S6 domain of Kv6.3 does not have the same regulatory effect as that of Kv8.1 (Fig. 8*C*, Table 1).

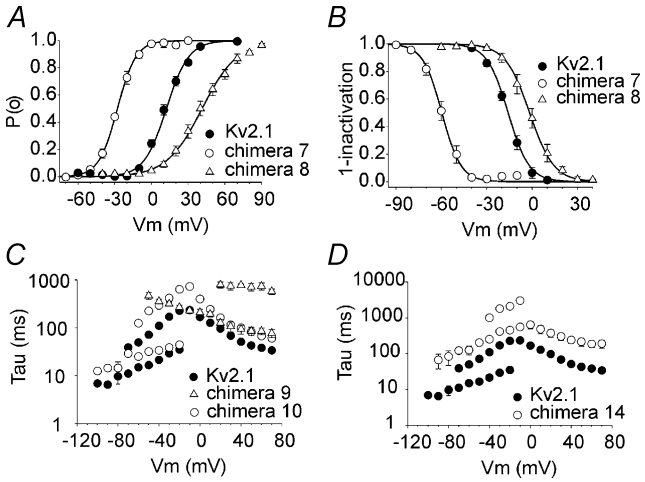

Figure 6. Voltage dependence of activation and inactivation
A, voltage dependence of activation. The activation curves of Kv2.1, chimeras 7 and 8 were obtained from the normalized initial tail amplitude recorded at −30 mV after 500 ms prepulses ranging from −80 mV to 70 mV in 10 mV steps. The continuous line represents the Boltzmann function fitted to the experimental data (see Methods). *B*, voltage dependence of inactivation. The inactivation curves of Kv2.1, chimeras 7 and 8 were obtained by the normalized peak currents recorded during a 250 ms test pulse to 50 mV plotted as a function of the 5 s prepulse ranging from −100 mV to 40 mV. Experimental data were fitted with a Boltzmann function (continuous lines). *C*, kinetics of activation and deactivation of Kv2.1 and chimeras 9 and 10. Time constants of activation and deactivation are plotted as a function of the test potential. To obtain the time constants for activation, test pulses were applied ranging from −10 mV to 70 mV for Kv2.1 and chimera 10, 500 ms in duration. For chimera 9 a 2 s. prepulse of −120 mV was given to recover from inactivation followed by test pulses ranging from −50 mV to 70 mV in 10 mV steps, 3 s in duration. To obtain the time constants for deactivation, a 200 ms prepulse to 50 mV was followed by test pulses ranging from −20 mV to −100 mV in 10 mV steps, 3 s in duration. The experimental data were fitted with mono- or double exponential functions, as appropriate. *D*, kinetics of activation and deactivation of Kv2.1 and chimera 14. Mean time constants ± S.E.M. of activation and deactivation are shown as a function of the step potentials. The pulse protocols for Kv2.1 are the same as in *C*. For chimera 14, test pulses for activation were applied ranging from 0 mV to 70 mV in 10 mV steps, 1 s in duration. To obtain the time constants for deactivation, a 500 ms prepulse to 50 mV was followed by test pulses ranging from −10 mV to −100 mV in 10 mV steps, 10 s in duration.

Discussion

The subunits from the Kv5–Kv11 subfamilies (Kv5.x, Kv6.x, Kv8.*x* and Kv9.x in the proposed IUPHAR convention)

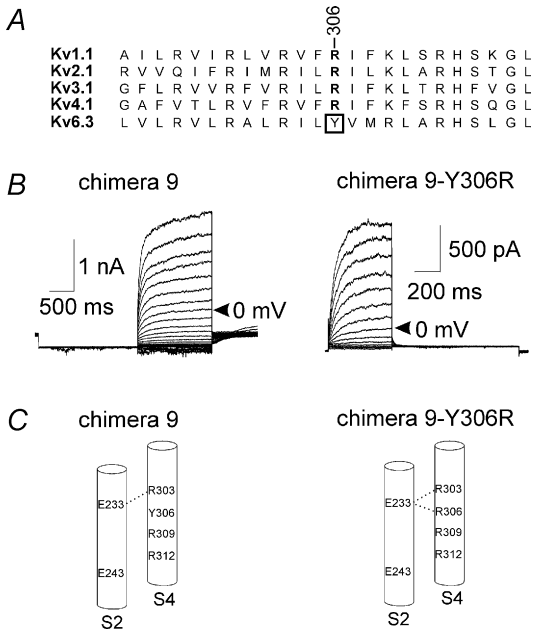

Figure 7. The S4 domain of Kv6.3
A, alignment of the S4 segment of Kv6.3 and one member of each functional subfamily. The conserved arginine is in bold and Y306 of Kv6.3 is boxed. *B*, typical recordings of chimera 9 (left) and the mutation Y306R (right). For chimera 9, the holding potential was −40 mV. A 2 s. prepulse of −120 mV was given to recover from inactivation, followed by depolarizing steps in 10 mV increments from −60 mV to +70 mV, 1.5 s in duration. For chimera 9–Y306R, the holding potential was −80 mV and cells were depolarized in 10 mV increments from −60 mV to +70 mV, 500 ms in duration, followed by a repolarizing pulse at −40 mV, 1 s in duration. For both chimeras, the trace at 0 mV is indicated by an arrow. *C*, S2 and S4 segments of chimera 9 (left) and the mutation Y306R (right). The proposed salt bridges between S2 and S4 are indicated by a dotted line.

are electrically silent, a property not unique to these subfamilies. Indeed, a G-protein-activated inward rectifying K^+ channel (GIRK3), a cyclic nucleotide-gated channel (HCN3) and hERG-USO are also electrically silent when expressed by themselves (Chen *et al.* 1993; Duprat *et al.* 1995; Kupershmidt *et al.* 1998). The subunits of the silent Kv subfamilies are incapable of forming functional homotetrameric channels, and remain in the ER when they are expressed in mammalian cells (Salinas *et al.* 1997*a*,*b*; Shepard & Rae, 1999; Ottschytsch *et al.* 2002). Even adding an established ER export signal (Ma *et al.* 2001) was not sufficient to rescue Kv6.3 out of the ER.

Many factors can cause ER retention. The amino terminus of Kv subunits contains a NAB domain, which is responsible for the subfamily-specific tetramerization (Li *et al.* 1992; Shen & Pfaffinger, 1995; Xu *et al.* 1995; Papazian, 1999). It was demonstrated for several silent Kv channels, including Kv6.3, that the amino termini failed to interact (Post *et al.* 1996; Kramer *et al.* 1998; Zhu *et al.* 1999; Ottschytsch *et al.* 2002). Given the fact that tetramerization of Kv channels occurs in the ER (Nagaya & Papazian, 1997; Lu *et al.* 2001), it is plausible to assume that Kv6.3 subunits are not capable of forming homotetramers and are consequently retained in the ER. However, replacing the N-terminal end of Kv6.3 by the Kv2.1 sequence did not rescue Kv6.3 out of the ER, despite the fact that Kv2.1 displays excellent trafficking. This finding indicates that additional factors must be responsible for ER retention, but does not exclude that Kv6.3 fails to tetramerize. Indeed, Kerschensteiner *et al.* (2005) showed recently that Kv9.3 (another silent subunit that interacts with Kv2.1), does not associate in a homomeric fashion inside mammalian cells. Some Kv channels were still functional after deletion of the NAB domain (VanDongen *et al.* 1990; Lee *et al.* 1994; Tu *et al.* 1996; Kobertz & Miller, 1999), indicating that other factors also determine tetramerization of subunits. This further indicates that the core domain (S1–S6) can form tetramers, and that the NAB domain exerts a dominant negative effect, prohibiting heteromerization between the subunits belonging to different Kv1 to Kv4 classes (Shen & Pfaffinger, 1995).

ER retention could also be caused by the presence of ER retention signals or the lack of export signals. Several signals have been shown to prevent channels from reaching

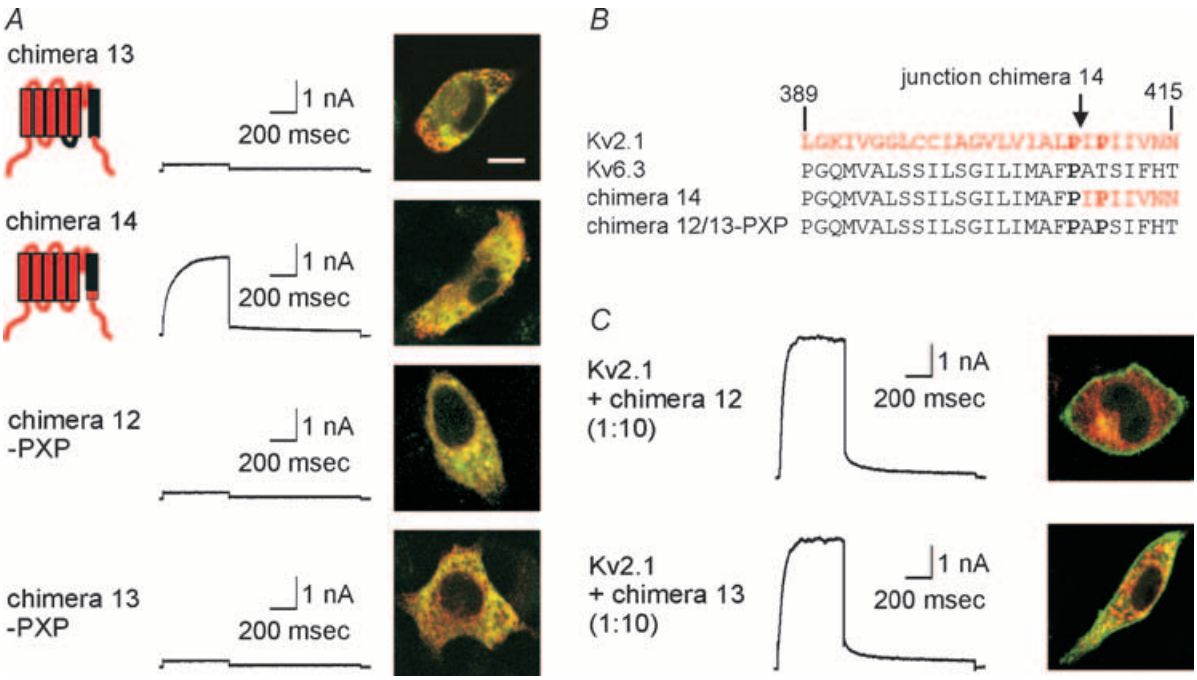

Figure 8. The S6 domain of Kv6.3
A, subcellular localization and typical current traces of chimeras 13, 14 and chimera 12–PXP. Currents were evoked by stepping from −80 mV to +70 mV, 500 ms in duration, followed by a repolarizing pulse at −30 mV, 1 s in duration. The confocal images show an overlay of the GFP-tagged constructs and DsRED-ER. The scale bar on the image represents 5 μm. *B*. alignment of the S6 segment of Kv2.1, Kv6.3, chimera 14 and chimera 12–PXP. Kv2.1 numbering is used. The prolines belonging to the P-X-P motif are in bold. The position of the junction in chimera 14 is indicated by an arrow. *C*, co-expressions of Kv2.1 with chimeras 12 and 13. For patch-clamp experiments, a 1 : 10 ratio of Kv2.1 and chimera was used to ensure the formation of heterotetramers. The same protocol as in *A* was used to evoke currents. For the confocal imaging, a 10 : 1 ratio of unlabelled Kv2.1 and GFP-tagged chimera was used.

the plasma membrane: KDEL, KKXX, RXR (Munro & Pelham, 1987; Jackson *et al.* 1990; Zerangue *et al.* 1999). In this case, tetramerization of Kv6.3 with Kv2.1 could mask such signals, allowing the heteromeric channel to leave the ER. Our results show that the ER retention of Kv6.3 was not caused by ER retention signals in the intracellular termini, since replacing the N- and C-terminus of Kv6.3 by the Kv2.1 sequence did not restore the trafficking.

The transmembrane domains of Kv6.3 did not contain dominant retention signals and did not cause folding problems since each domain could replace the corresponding Kv2.1 domain, with the exception of S6. Similar results were obtained for Kv8.1 and Kv1.3 (Hugnot *et al.* 1996). For Kv8.1 it was shown that the S6 segment was responsible for the modulatory effect of Kv8.1 on Kv2.1 (Salinas *et al.* 1997*a*). For Kv6.3, our data do not support such role (Fig. 8*C*). However, all known silent Kv channels lack the second proline of the highly conserved P-X-P motif, probably resulting in a structure that differs from the one of the functional Kv channels, as the P-X-P motif is assumed to bend the helix (del Camino *et al.* 2000; Labro *et al.* 2003). Although the S6 domain of Kv6.3 was not functional in a Kv2.1 background, this could not be the sole reason for the ER retention of Kv6.3. In an attempt to restore the function of Kv6.3, we introduced the ion-conducting domain of Kv2.1 in Kv6.3 (chimera 4). Since this chimera (containing the S6 domain of Kv2.1) was also unable to produce current, there has to be an additional reason for the non-functionality besides the incompatible S6 domain.

The pore loop of Kv6.3 (chimera 11) caused ER retention, as we never observed plasma membrane staining, but the chimera was still able to produce voltage-gated K^+ current, indicating that the retention was not complete. Chimera 11 displayed a lower normalized peak amplitude compared to the chimeras that showed plasma membrane staining (∼6–12 times less current) demonstrating the reduction of the number of channels at the level of the plasma membrane. In general, robust expression coincides with clear peripheral staining. In cases of low expression, the patch-clamp approach appears to be more sensitive than standard confocal imaging of GFP-tagged subunits. Indeed, a 100 pA voltage-dependent outward current at +60 mV is clearly identifiable in L-cells, but this represents approximately 100 channels in the whole cell (∼10 pS, 150 mV driving force, $P(o) \sim 0.7$) (Hartmann *et al.* 1991; Benndorf *et al.* 1994). A typical confocal slice contains only 5–10% of the total plasma membrane area (depending on the level in the stack), or only 5–10 channels, which would be difficult to detect as convincing peripheral staining (plasma membrane) in comparison with the fluorescence of a large number of subunits in the ER.

Interestingly, the S4 segment of Kv6.3 in Kv2.1 still acted as a voltage sensor but the voltage dependence of activation and inactivation was shifted to extremely negative potentials (chimera 9). All functional Kv channels contain a conserved arginine (R371 in *Shaker*), whereas in Kv6.3 a tyrosine is present at this position. It was previously shown that neutralization of this arginine in *Shaker* leads to hyperpolarizing shifts in the mid-point of activation (Papazian *et al.* 1991; Miller & Aldrich, 1996). This arginine has been proposed to form a salt bridge with a glutamic acid in S2 (Fig. 7*C*; Tiwari-Woodruff *et al.* 1997). Indeed, mutation of the tyrosine to an arginine restored the voltage dependence of activation and inactivation of chimera 9–Y306R close to normal. This observation demonstrates the importance of this charge network between S2 and S4 in Kv6.3, and suggests a general mechanism in Kv channels, including silent channels. The specific subunit composition of the heterotetrameric Kv2.1/Kv6.3 channel is not known, but clearly contains at least one Kv6.3 subunit, hence at least one S4 of Kv6.3 (Kerschensteiner *et al.* 2005). As such, the shifted voltage dependence of activation and inactivation of the Kv2.1/Kv6.3 heterotetramer (Ottschytsch *et al.* 2002) could reflect the gating behaviour of the Kv6.3 subunit. Furthermore it is of interest that the S2 chimera (chimera 7) displayed a voltage dependence of inactivation similar to the Kv6.3/Kv2.1 heterotetramers, consistent with a role for the S2–S4 charge network.

In conclusion, the ER retention of Kv6.3 is not due to the NAB domain, which is unable to form homotetramers, nor to the absence or presence of trafficking signals in its N- or C-terminus. Each transmembrane domain of Kv6.3 was functional in a Kv2.1 background, with the exception of the full S6. Furthermore, we could demonstrate that the lack of the conserved arginine at position 306 in the S4 domain of Kv6.3 is responsible for the hyperpolarizing shift of activation and inactivation. This study suggests that the silent behaviour of Kv6.3 is largely caused by the C-terminal part of its sixth transmembrane domain that causes ER retention of the subunit.

References

Barry DM & Nerbonne JM (1996). Myocardial potassium channels: electrophysiological and molecular diversity. *Annu Rev Physiol* **58**, 363–394.

Benndorf K, Koopmann R, Lorra C & Pongs O (1994). Gating and conductance properties of a human delayed rectifier K^+ channel expressed in frog oocytes. *J Physiol* **477**, 1–14.

Bezanilla F (2000). The voltage sensor in voltage-dependent ion channels. *Physiol Rev* **80**, 555–592.

Chen J, Mitcheson JS, Tristani-Firouzi M, Lin M & Sanguinetti MC (2001). The S4–S5 linker couples voltage sensing and activation of pacemaker channels. *Proc Natl Acad Sci U S A* **98**, 11277–11282.

Chen TY, Peng YW, Dhallan RS, Ahamed B, Reed RR & Yau KW (1993). A new subunit of the cyclic nucleotide-gated cation channel in retinal rods. *Nature* **362**, 764–767.

Decher N, Chen J & Sanguinetti MC (2004). Voltage-dependent gating of hyperpolarization-activated, cyclic nucleotide-gated pacemaker channels: molecular coupling between the S4–S5 and C-linkers. *J Biol Chem* **279**, 13859–13865.

del Camino D, Holmgren M, Liu Y & Yellen G (2000). Blocker protection in the pore of a voltage-gated K^+ channel and its structural implications. *Nature* **403**, 321–325.

Drewe JA, Verma S, Frech G & Joho RH (1992). Distinct spatial and temporal expression patterns of K^+ channel mRNAs from different subfamilies. *J Neurosci* **12**, 538–548.

Duprat F, Lesage F, Guillemare E, Fink M, Hugnot JP, Bigay J, Lazdunski M, Romey G & Barhanin J (1995). Heterologous multimeric assembly is essential for K^+ channel activity of neuronal and cardiac G-protein-activated inward rectifiers. *Biochem Biophys Res Comms* **212**, 657–663.

Gaynor EC, Graham TR & Emr SD (1998). COPI in ER/Golgi and intra-Golgi transport: do yeast COPI mutants point the way? *Biochim Biophys Acta* **1404**, 33–51.

Gong Q, Anderson CL, January CT & Zhou Z (2002). Role of glycosylation in cell surface expression and stability of HERG potassium channels. *Am J Physiol Heart Circ Physiol* **283**, H77–H84.

Hamill OP, Marty A, Neher E, Sakmann B & Sigworth FJ (1981). Improved patch clamp techniques for high-resolution current recording from cells and cell-free membrane patches. *Pflugers Archl* **391**, 85–100.

Hartmann HA, Kirsch GE, Drewe JA, Taglialatela M, Joho RH & Brown AM (1991). Exchange of conduction pathways between two related K^+ channels. *Science* **251**, 942–944.

Heginbotham L, Lu Z, Abramson T & MacKinnon R (1994). Mutations in the K^+ channel signature sequence. *Biophys J* **66**, 1061–1067.

Hille B (2001). *Ion Channels of Excitable Membranes*, 3rd edn. Sinauer, Sunderland, MA.

Hugnot JP, Salinas M, Lesage F, Guillemare E, de Weille J, Heurteaux C, Mattei MG & Lazdunski M (1996). Kv8.1, a new neuronal potassium channel subunit with specific inhibitory properties towards *Shab* and *Shaw* channels. *EMBO J* **15**, 3322–3331.

Jackson MR, Nilsson T & Peterson PA (1990). Identification of a consensus motif for retention of transmembrane proteins in the endoplasmic reticulum. *EMBO J* **9**, 3153–3162.

Kerschensteiner D, Soto F & Stocker M (2005). Fluorescence measurements reveal stoichiometry of K^+ channels formed by modulatory and delayed rectifier alpha-subunits. *Proc Natl Acad Sci U S A* **102**, 6160–6165.

Kobertz WR & Miller C (1999). K^+ channels lacking the 'tetramerization' domain: implications for pore structure. *Nature Structural Biol* **6**, 1122–1125.

Kramer JW, Post MA, Brown AM & Kirsch GE (1998). Modulation of potassium channel gating by coexpression of Kv2.1 with regulatory Kv5.1 or Kv6.1 alpha-subunits. *Am J Physiol* **274**, C1501–C1510.

Kupershmidt S, Snyders DJ, Raes AR & Roden D (1998). A K^+ channel splice variant common in human heart lacks a C-terminal domain required for expression of rapidly-activating delayed rectifier current. *J Biol Chem* **273**, 27231–27235.

Labro AJ, Raes AL, Bellens I, Ottschytsch N & Snyders DJ (2003). Gating of *Shaker*-type channels requires the flexibility of S6 caused by prolines. *J Biol Chem* **278**, 50724–50731.

Lee TE, Philipson LH, Kusnetsov A & Nelson DJ (1994). Structural determinant for assembly of mammalian K^+ channels. *Biophys J* **66**, 667–673.

Letourneur F, Gaynor EC, Hennecke S, Demolliere C, Duden R, Emr SD, Riezman H & Cosson P (1994). Coatomer is essential for retrieval of dilysine-tagged proteins to the endoplasmic reticulum. *Cell* **79**, 1199–1207.

Li M, Jan YN & Jan LY (1992). Specification of subunit assembly by the hydrophilic amino- terminal domain of the *Shaker* potassium channel. *Science* **257**, 1225–1230.

Lu J, Robinson JM, Edwards D & Deutsch C (2001). T1–T1 interactions occur in ER membranes while nascent Kv peptides are still attached to ribosomes. *Biochemistry* **40**, 10934–10946.

Ma D, Zerangue N, Lin YF, Collins AYuM, Jan YN & Jan LY (2001). Role of ER export signals in controlling surface potassium channel numbers. *Science* **291**, 316–319.

Margeta-Mitrovic M, Jan YN & Jan LY (2000). A trafficking checkpoint controls GABA (B) receptor heterodimerization. *Neuron* **27**, 97–106.

Miller AG & Aldrich RW (1996). Conversion of a delayed rectifier K^+ channel to a voltage-gated inward rectifier K^+ channel by three amino acid substitutions. *Neuron* **16**, 853–858.

Munro S & Pelham HR (1987). A C-terminal signal prevents secretion of luminal ER proteins. *Cell* **48**, 899–907.

Nagaya N & Papazian DM (1997). Potassium channel alpha and beta subunits assemble in the endoplasmic reticulum. *J Biol Chem* **272**, 3022–3027.

Ottschytsch N, Raes A, Van Hoorick D & Snyders DJ (2002). Obligatory heterotetramerization of three previously uncharacterized Kv channel alpha -subunits identified in the human genome. *Proc Natl Acad Sci U S A* **99**, 7986–7991.

Papazian DM (1999). Potassium channels: some assembly required. *Neuron* **23**, 7–10.

Papazian DM, Timpe LC, Jan YN & Jan LY (1991). Alteration of voltage-dependence of *Shaker* potassium channel by mutations in the S4 sequence. *Nature* **349**, 305–310.

Patel AJ, Lazdunski M & Honore E (1997). Kv2.1/Kv9.3, a novel ATP-dependent delayed-rectifier K^+ channel in oxygen-sensitive pulmonary artery myocytes. *EMBO J* **16**, 6615–6625.

Patel AJ, Lazdunski M & Honore E (1999). Kv2.1/Kv9.3, an ATP-dependent delayed-rectifier K^+ channel in pulmonary artery myocytes. *Ann N Y Acad Sci* **868**, 438–441.

Pongs O (1999). Voltage-gated potassium channels: from hyperexcitability to excitement. *FEBS Lett* **452**, 31–35.

Post MA, Kirsch GE & Brown AM (1996). Kv2.1 and electrically silent Kv6.1 potassium channel subunits combine and express a novel current. *FEBS Lett* **399**, 177–182.

Salinas M, de Weille J, Guillemare E, Lazdunski M & Hugnot JP (1997*a*). Modes of regulation of shab K^+ channel activity by the Kv8.1 subunit. *J Biol Chem* **272**, 8774–8780.

Salinas M, Duprat F, Heurteaux C, Hugnot JP & Lazdunski M (1997*b*). New modulatory alpha subunits for mammalian *Shab* K^+ channels. *J Biol Chem* **272**, 24371–24379.

Shen NV & Pfaffinger PJ (1995). Molecular recognition and assembly sequences involved in the subfamily-specific assembly of voltage-gated K^+ channel subunit proteins. *Neuron* **14**, 625–633.

Shepard AR & Rae JL (1999). Electrically silent potassium channel subunits from the human lens epithelium. *Am J Physiol* **277**, C412–C424.

Thorneloe KS & Nelson MT (2003). Properties and molecular basis of the mouse urinary bladder voltage-gated K^+ current. *J Physiol* **549**, 65–74.

Tiwari-Woodruff SK, Schulteis CT, Mock AF & Papazian DM (1997). Electrostatic interactions between transmembrane segments mediate folding of *Shaker* K^+ channel subunits. *Biophys J* **72**, 1489–1500.

Tristani-Firouzi M, Chen J & Sanguinetti MC (2002). Interactions between S4–S5 linker and S6 transmembrane domain modulate gating of HERG K^+ channels. *J Biol Chem* **277**, 18994–19000.

Tu LW, Santarelli V, Sheng ZF, Skach W, Pain D & Deutsch C (1996). Voltage-gated K^+ channels contain multiple intersubunit association sites. *J Biol Chem* **271**, 18904–18911.

VanDongen AM, Frech GC, Drewe JA, Joho RH & Brown AM (1990). Alteration and restoration of K^+ channel function by deletions at the N- and C-termini. *Neuron* **5**, 433–443.

Xu J, Yu W, Jan YN, Jan LY & Li M (1995). Assembly of voltage-gated potassium channels. *J Biol Chem* **270**, 24761–24768.

Zerangue N, Schwappach B, Jan YN & Jan LY (1999). A new ER trafficking signal regulates the subunit stoichiometry of plasma membrane K(ATP) channels. *Neuron* **22**, 537–548.

Zhu XR, Netzer R, Bohlke K, Liu Q & Pongs O (1999). Structural and functional characterization of Kv6.2 a new gamma-subunit of voltage-gated potassium channel. *Receptors Channels* **6**, 337–350.

Acknowledgements

We would like to thank Tessa de Block, Evy Mayeur, Carole Faghel and Tine Bruyns for their excellent technical assistance. This work was supported by the 'Vlaams Interuniversitair Instituut voor Biotechnologie' Grant VIB PRJ05, the Interuniversity Attraction Poles program P5/19 of the Belgian Federal Science Policy Office, the 'Fonds voor Wetenschappelijk Onderzoek Vlaanderen' Grant FWO-G0421.02, a concerted research project Grant GOA 2004 of the University of Antwerp and the NHLBI National Institutes of Health Grant HL59689.